



Article

Commercial Arthrospira platensis Extract Modifies the Photophysiology of Cladocopium goreaui, Coral Endosymbiont Microalgae

Thibault Le Verge-Campion 1,* D, Thierry Jauffrais 1D, Luc Lefeuvre 2 and Fanny Houlbrèque 1D

- ENTROPIE, IRD, Ifremer, Université de la Nouvelle-Calédonie, Univ La Réunion, CNRS, UMR 9220 ENTROPIE, 98800 Nouméa, New Caledonia; thierry.jauffrais@ifremer.fr (T.J.); fanny.houlbreque@ird.fr (F.H.)
- ² Laboratoires Dermatologiques d'Uriage, 92200 Neuilly-Sur-Seine, France; luc.lefeuvre@uriage.fr
- * Correspondence: thibault.leverge@gmail.com

Abstract

Arthrospira platensis extract is incorporated into sunscreen formulations for its beneficial and UV-protective properties on cultured human cells. However, its effects have not yet been assessed on non-target organisms such as endosymbiotic microalgae in coral tissue. To evaluate its effects, we investigated the photophysiology of the cultured dinoflagellate Cladocopium goreaui using PAM fluorometry (RLC, OJIP) after a 5-day exposure to different extract concentrations. Our results show that, through a hormetic effect, A. platensis enhances the performance index (Pi_Abs) at 0.018 mg L $^{-1}$ by increasing the number of active reaction centers (RC/ABS) and improving electron transfer efficiency (ϕ Eo, ψ Eo) along the electron transport chain. Conversely, beyond 108.8 mg L $^{-1}$, negative impacts appear on PSII, increasing the apparent antenna size (ABS/RC) and impairing the oxygenevolving complex (K-peak), ultimately reducing the maximum relative electron transport rate (rETR_m). This relative toxicity, obtained only for the highest concentrations, supports its potential incorporation into cosmetic formulations. This study contributes to improving the ecotoxicity assessment of cosmetic products on non-target organisms.

Keywords: Arthrospira platensis; Cladocopium goreaui; photophysiology; dose–response relationship; JIP-test; coral



Academic Editor: Adele Cutignano

Received: 22 April 2025 Revised: 6 June 2025 Accepted: 25 June 2025 Published: 22 September 2025

Citation: Le Verge-Campion, T.; Jauffrais, T.; Lefeuvre, L.; Houlbrèque, F. Commercial *Arthrospira platensis* Extract Modifies the Photophysiology of *Cladocopium goreaui*, Coral Endosymbiont Microalgae. *Phycology* 2025, 5, 50. https://doi.org/10.3390/ phycology5030050

Copyright: © 2025 by the authors. Licensee MDPI, Basel, Switzerland. This article is an open access article distributed under the terms and conditions of the Creative Commons Attribution (CC BY) license (https://creativecommons.org/licenses/by/4.0/).

1. Introduction

Coral reefs are the most impressive biomineral production on the planet. The longevity and spatial extension of corals are largely due to the existence within their endodermal cells of symbiotic microalgae, belonging to the family Symbiodiniaceae [1] and capable of photosynthesis [2]. Extreme coral reef biodiversity, comparable to that of tropical forests, contributes to the economic development of more than a hundred countries that enjoy them along their coasts [3]. Nowadays, in addition to the impact of global warming, coral reefs are threatened by multiple stressors [4,5] including pharmaceutical pollution from direct bathing or indirect releases into the environment [6].

In recent years, more and more pharmaceutical and personal care products (PCPs) have been released into the environment [7]. The presence and persistence of their residues, with active biological action, contribute to create pan-global contamination [8]. Those residues can be detected in all areas of the globe, ranging from urban areas to estuaries, including polar zones [9], temperate zones [10], or tropical waters [11–13]. Among these PCPs, certain ultra-violet filters (UVFs) incorporated in sunscreen products are responsible

Phycology **2025**, 5, 50 2 of 16

for various harmful effects on corals, altering their metabolism [14] and physiology [15–19] and ultimately leading to coral bleaching [20], the expulsion of the symbiotic microalgae from coral gastrodermal cells. Under normal conditions, through photosynthesis, these Symbiodiniaceae provide the coral host with most of its energy requirements [21]. However, under stressful conditions, photosynthetic mechanisms are disrupted, leading to an excessive production of reactive oxygen species (ROS), toxic to the host [22], causes the Symbiodiniaceae to be expelled. Most studies on UVFs have, however, focused on their direct impact on corals [13,23] rather than on their symbiotic algae. However, Vuckovic et al. [24] have demonstrated that UVF metabolites can also have adverse effects on coral symbionts.

In order to develop environmentally safer sunscreen products containing UVFs, refining formulations is crucial to minimize their impact on organisms. Recent studies suggest that the addition of natural substances could help organisms cope with abiotic stress. Microalgal extracts, both marine or freshwater, are of interest due to their composition involving pigments (carotenoids, phycoerythrin, phycocyanin), nutrients, and antioxidants, as well as UV-absorbing compounds. Already used in pharmaceutical and agronomic industries, algae extracts demonstrate beneficial effects through their antioxidant and protective properties, as well as their role as biostimulants for cultures such as cereals and vineyards, increasing both plant quality and yield [25]. Commercialized as powders or aqueous extracts with the objective of being incorporated into commercial cosmetic formulations, these substances require evaluation of their impacts on model or non-target organisms.

To date, there have been very few studies on the impact of these substances on corals and particularly on symbionts, the most sensitive stage of coral physiology [26,27]. This study investigates the effects of an algal-based extract derived from the cyanobacterium *Arthrospira platensis* containing phycocyanin (PC), applied at different concentrations to the *ex hospite* dinoflagellate *Cladocopium goreaui*. *Cladocopium* is considered the most dominant genus of symbiotic dinoflagellates in the Indo-Pacific region [1,28] with *C. goreaui* being a representative symbiont in New Caledonia [28,29]. In addition, *C. goreaui* is well cultivated under laboratory conditions [30,31], making it a relevant model for ecotoxicological assessments [27,31,32]. More specifically, this study aims to assess the effects of this extract on the growth, photophysiological capacities, activity, and functioning of photosystems, as well as on the efficiency of the electron acceptor intersystem of *C. goreaui*. We focus in particular on the fluorescent transient analysis (OJIP), a fast, accurate, and non-invasive method for characterizing photosystem structure, as well as electron transfers within organisms exposed to abiotic stress [33,34].

2. Materials and Methods

2.1. Arthrospira Platensis Extract and Concentration Exposure

The extract tested in this study was purchased from GreenTech (SAS GREENSEA, Saint-Beauzire, France). This extract was composed of *Arthrospira platensis* (CAS n° 223751-80-2; estimated 1–10%) diluted in glycerin (CAS n° 56-81-5; estimated 75–90%) and water (CAS n° 7733-18-5; estimated 10–20%). The phycocyanin concentration was measured at 1.1 g L $^{-1}$ according to the certificate of analyses provided by the manufacturer. A diluted stock solution of the complete commercial extract was prepared at 1.6 g L $^{-1}$ in filtered seawater (FSW, 0.2 μ m) [31] enriched with L1 media and stored in the dark at 4 °C.

Exposure concentrations were chosen based on three studies estimating the amount of total sunscreen released into seawater during a summer day [35–37]. Predicted environmental sunscreen concentration was obtained as follows: $PEC_{Sunscreen} = (N \times B \times SA \times m)/V$ (1) with N: the number of people on the beach (here fixed at 3000), B: the percentage of people applying sunscreen before bathing (47%), SA: average number of sunscreen

Phycology **2025**, 5, 50 3 of 16

applications per person (2.4), m: the amount of sunscreen applied per person and per application (15 g pers $^{-1}$), and V: the seawater turnover near the beach (5850 m 3). These parameters were set according to Ficheux et al. [38] and Labille et al. [35]. PEC_{Extract} was obtained by multiplying PEC_{Sunscreen} by the fraction of the extract (%Extract) in the used formulation: PEC_{Extract} = PEC_{Sunscreen} \times %Extract (2) (% extract = 0.2% [39]). Finally, PEC_{Extract} was estimated to 0.016 mg L $^{-1}$ in seawater and corresponds to the lowest dose of the study (LD). To assess the potential effects of the substance at higher concentrations, three additional doses were selected: Medium Dose (MD), High Dose (HD), and Extreme Dose (ED), at 0.16 mg L $^{-1}$, 1.6 mg L $^{-1}$, and 1600 mg L $^{-1}$, respectively. An additional experiment conducted using glycerol at equivalent concentrations (except ED) showed no significant impact on the growth or photophysiology (OJIP, RLC) of *C. goreaui* (Supplementary Materials Tables S1 and S2).

2.2. Microalgal Culture

Marine microalgae *Cladocopium goreaui* (SCF055.01-10, WT10) were purchased from the Australian Institute of Marine Sciences (AIMS, Townsville, Australia). Cultures were maintained in filtered seawater (0.2 μ m, salinity 35) enriched with L1 media [40] at 26 °C in a thermostatic chamber. A day: night cycle was respected following a 14 h:10 h ratio, with an irradiance of 70 \pm 10 μ mol photons m⁻² s⁻¹. Culture renewal was operated every 3 weeks to maintain the microalgae in exponential growth [31,41].

Microalgae growth cultures were run in triplicates using 250 mL sterilized glass flasks filled with FSW enriched in L1 media. The necessary volume of the extract stock solution was added to the conical flasks to reach the exposure concentrations (LD, MD, HD and ED) with a final volume of 150 mL. The initial cell concentration in each flask was $3.5 \cdot 10^5$ cell mL⁻¹. Flasks were sampled daily (2 mL) for 20 days to perform fluorometric assessments. During the experiment, flasks were randomized daily to ensure similar light conditions [31].

2.3. Physiological Measurements on Algae

2.3.1. Growth Analysis

Growth was followed using two complementary methods. Cell enumeration was performed using cell counts on a Nageotte hemocytometer under optical microscopy (Leica DM750, Leïca Microsystems, Wetzlar, Germany) while minimal fluorescence (F_0) was measured by pulse amplitude modulation (PAM) fluorometry (AquaPen-C AP 110-C, Photon Systems Instruments, Dràsov, Czech Republic). To enhance the precision and repeatability of cell measurements, a proxy was created based on cell counts on a hemocytometer and F_0 measurements (Supplementary Materials Figure S1). A Gompertz model was fitted to the data to assess the maximum growth rate (μ max in days $^{-1}$), the maximum cell concentration (A in log(C - C₀)), and the latency time (λ in days) [42,43]:

$$F(t) = A \times \exp(-\exp(\mu_{\text{max}} \times \exp(1)/\alpha \times (\lambda - t) + 1)). \tag{1}$$

2.3.2. PAM Fluorometry

Photosynthetic parameters were measured using a PAM fluorometer (AquaPen-C AP 110-C, Photon Systems Instruments, Dràsov, Czech Republic) equipped with a blue light- emitting diode at 470 nm. All samples were first dark-adapted for 15 min to ensure oxidized (open) PSII reactional centers, then homogenized before measurements at room temperature. Rapid Light Curves (RLCs), allowing one to evaluate the light utilization at different intensities, were generated by illuminating samples with 7 increasing light steps (10, 20, 50, 100, 300, 500, and 1000 μ mol photons m⁻² s⁻¹) [44]. The Jassby and Platt model [45] was used to fit the RLCs and estimate quantitative parameters: rETR_m, alpha

Phycology **2025**, 5, 50 4 of 16

(α), and Ek. RLCs were also used to calculate the Stern–Volmer coefficient indicating the non-photochemical quenching induced by light curve (NPQ_{ind}) [46].

To investigate more precisely the electron pathway within PSII, Fluorescence rise OJIP curves were recorded from 50 μ s to 2 s after a 2100 μ mol photons m⁻² s⁻¹ saturating pulse (corresponding to a 70% super pulse as recommended by the manufacturer) on the same dark-readapted and homogenized samples. Data were extracted and extrapolated according to Strasser et al. [33] to generate the parameters described in Appendix A.1 (Table A1). The OJIP transients were represented as the total fluorescence intensity (F_t) plotted on a logarithmic time scale from O-step (50 μ s) to P-step (here considered as F_m) [33] to ensure a sufficient signal prior to analysis. F_t was double-normalized by F₀ and F_m to plot the variable fluorescence (V_t) over time V_t = (F_t - F₀)/(F_m - F₀) to compare signals with different intensities. V_t can also be plotted between each biophysical step to further analyze a specific phase (OJ, OI, JI or IP) as W_(YZ) = (F_t - F_Y)/(F_Z - F_Y). Finally, each parameter was normalized with the control as Δ W_{(YZ)t} = [W_{(YZ)Treated}]_t - [W_{(YZ)Control}]_t to reveal potential hidden treatment impacts [47]. W_k, corresponding to a specific time, is obtained at t₃₀₀: (F₃₀₀ - F₀)/(F_i - F₀) = V_k/V_i, and represented in function of F_v/F_m.

2.4. Statistical Analyses

Statistical analyses were performed thanks to *RStudio* software (R Core Team 2017). Data were tested for normality and homoskedasticity using Shapiro–Wilk and Levene tests, respectively. One way ANOVA or Kruskal–Wallis tests were conducted to identify a concentration effect on parameters, followed by post-hoc analysis with Tukey HSD or the Dunn test. All data are presented as mean \pm SD with the significance level placed at $\alpha = 0.05$.

Pi_Abs was plotted as a percentage response relative to the control (control = 100%) as a function of the concentration logarithm. A linear model was tested to fit the data, then adjusted by adding a quadratic term to the model to improve the adjustment. The lowest Akaike Information Criterion (AIC) was used to identify the best model, and residuals were graphically assessed using a QQ-plot.

3. Results

3.1. Growth Rates

Cladocopium goreaui exhibited similar growth parameters (A, μ_{max} , and λ) for the control (CTL), low dose (LD), medium dose (MD), and high dose (HD) conditions (Table 1). In contrast, parameters for the extreme dose (ED) were reduced, with a 77% decrease in the maximum cell concentration (A) and a 45% decrease in the maximum growth rate (μ_{max}) (p < 0.01) compared to the control condition.

Table 1. Growth parameters extracted from the Gompertz model: A (log(C/C₀)), the maximum cell concentration (where C and C₀ are the final and initial cell concentrations, respectively); μ_{max} (days⁻¹), the maximum growth rate; and λ (days), the latency time. Values are expressed as mean \pm SD (n = 3). Different letters indicate statistically significant differences between treatments (p < 0.05): control (CTL), low dose (LD), medium dose (MD), high dose (HD), and extreme dose (ED).

	Α	μ_{max}	λ
CTL	$0.80\pm0.03~\mathrm{ab}$	$0.09\pm0.01~\mathrm{ab}$	2.25 ± 0.65 a
LD	$0.88\pm0.05~^{\mathrm{a}}$	0.09 ± 0.01 a	2.24 ± 0.37 a
MD	0.89 ± 0.07 a	0.08 ± 0.01 a	2.07 ± 0.62 a
HD	$0.77\pm0.03~\mathrm{ab}$	0.09 ± 0.00 $^{ m ab}$	2.04 ± 0.48 a
ED	$0.18 \pm 0.07^{\text{ b}}$	$0.05 \pm 0.02^{\text{ b}}$	2.23 ± 0.50 a

Phycology **2025**, 5, 50 5 of 16

3.2. Chlorophyll Fluorescence Signal After 5 Days Exposure

3.2.1. Rapid Light Curves

There was no difference in the maximum relative electron transport rate (rETR_m) between CTL, LD, MD, and HD treatments (Figure 1 and Table 2). A 33% reduction in rETR_m and a 22% reduction of Ik (the saturating light parameter) were observed in ED treatment. No difference in NPQ was observed in the non-photochemical quenching- (NPQ) induced parameter in all treatments (p > 0.05).

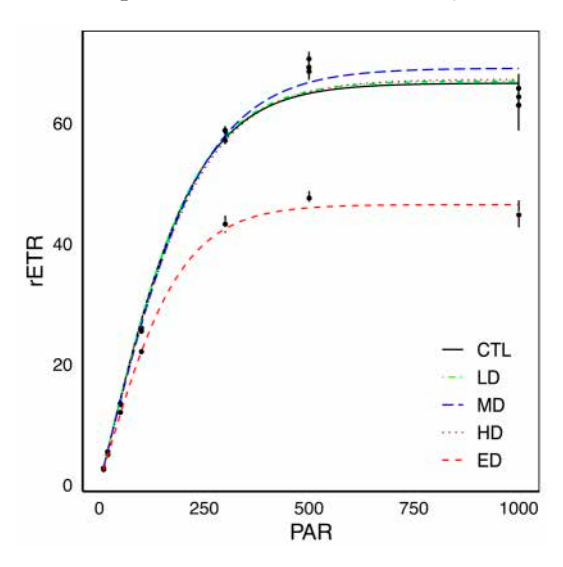


Figure 1. rETR of *C. goreaui* under increasing light intensities (PAR, μ mol photons m⁻² s⁻¹) exposed to different concentrations of *A. platensis* extract. Curves are fitted Rapid Light Curves (RLCs) modelized by Jassby and Platt model (1975). Control (CTL), low dose (LD), medium dose (MD), high dose (HD), and extreme dose (ED). Black dots are mean \pm SD (n = 3).

Table 2. Photophysiological parameters extracted from the fitted Rapid Light Curve (RLC) for increasing *A. platensis* extract concentrations. Values are mean \pm SD (n=3). Letters represent statistical differences between treatments: control (CTL), low dose (LD), medium dose (MD), high dose (HD), and extreme dose (ED). rETR_m: maximum relative electron transport rate; α: initial RLC slope; Ek: light-saturating index = rETR_m/α; NPQ_{ind}: non-photochemical quenching induced by the RLC.

	rETR _m	α	Ik	NPQ _{ind}
CTL	66.66 ± 0.61 ab	0.29 ± 0.00 a	228.15 ± 0.31 ab	0.29 ± 0.03 a
LD	67.04 ± 3.20 ab	0.29 ± 0.00 $^{\mathrm{ab}}$	230.98 ± 14.02 $^{\mathrm{ab}}$	0.31 ± 0.04 a
MD	69.15 \pm 1.14 $^{\mathrm{a}}$	0.28 ± 0.00 $^{\mathrm{ab}}$	242.17 \pm 8.13 $^{\mathrm{a}}$	0.36 ± 0.02 a
HD	$67.31\pm1.75~\mathrm{ab}$	0.28 ± 0.01 $^{ m ab}$	240.76 ± 6.75 a	0.38 ± 0.03 a
ED	46.52 ± 1.89 b	0.25 ± 0.00 b	188.38 ± 5.95 b	0.30 ± 0.02 a

3.2.2. Rapid Chl a Fluorescence Transient Analyses

Chl a contained in *C. goreaui* exhibited a typical fluorescent transient shape in each treatment, going from O-step (F_0) to P-step, including two intermediate steps: J-step and I-step (Figure 2a). The lowest signal intensity (F_t) was observed for the ED treatment (Figure 2a). The double normalized fluorescence ($V_t = (F_t - F_0)/(F_m - F_0)$) is presented in Figure 2b. Main variations were observed during the O-J phase (0 to 2 ms), with a slight reduction in V_j (corresponding to V_t at 2 ms) for the LD, MD, and HD treatments. A control normalized representation $\Delta W_{OP} = W_{OP[Sample]} - W_{OP[Control]}$ allowed a better identification of V_t variations compared to the control condition (Figure 3a). ΔW_{OP} amplitudes for LD, MD and HD were overall negatives during the O-J (0 to 2 ms) and J-I phases (2 to 30 ms) before becoming positives on the I-P-phase (30 ms to F_m). Only the ED treatment showed

Phycology **2025**, 5, 50 6 of 16

a positive amplitude during the O-J phase before returning to the control baseline at the J-step (V_j). To further the analysis of the O-J phase, a normalized representation against the control as $\Delta W_{OJ} = W_{OJ[Sample]} - W_{OJ[Control]}$ (Figure 3b) revealed a clear positive new band (or peak) near 300 μ s, characterized by a higher variable fluorescence in the ED treatment compared to control one ($V_{t[ED]} > V_{t[CTL]}$ at 300 μ s). This new band, generally hidden on a classic OJIP representation, corresponds to the "K-step" and gives an OKJIP shape to the fluorescence transient in the ED treatment, whereas other treatments revealed the classic OJIP shape. This K-peak amplitude was well defined for ED, as highlighted by the V_k/V_j ratio ($V_k/V_j > 0.6$), which differed notably from the other treatments ($V_k/V_j < 0.6$) (Figure 4).

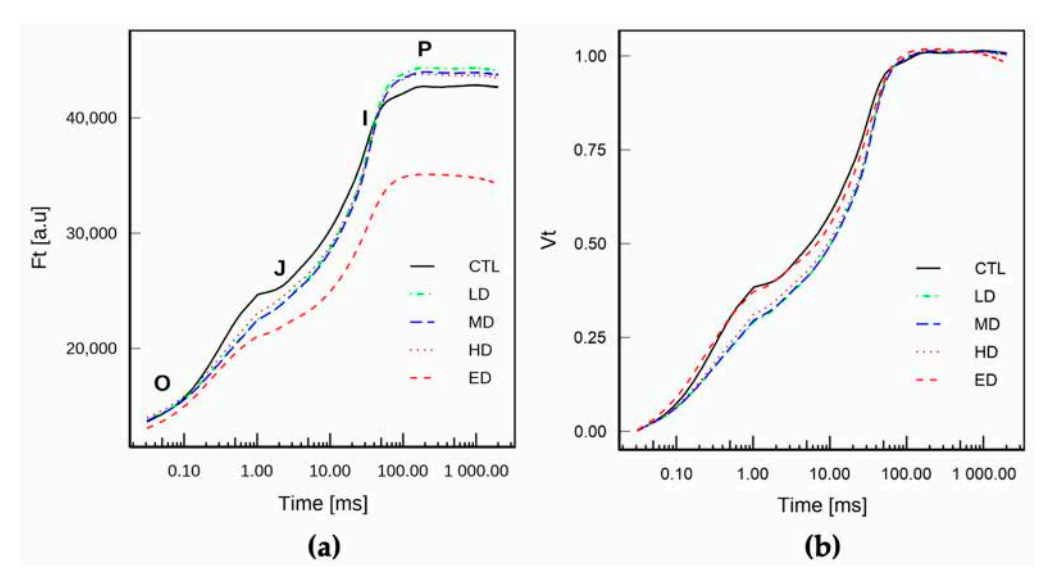


Figure 2. Fluorescent OJIP transients of dark-adapted *C. goreaui* exposed to different *A. platensis* extract concentrations: control (CTL); low dose (LD); medium dose (MD), high dose (HD), and extreme dose (ED). (a) Fluorescence (F_t) at t time and (b) relative variable fluorescence (V_t), double normalized on F_m and F_0 as $V_t = (F_t - F_0)/(F_m - F_0)$.

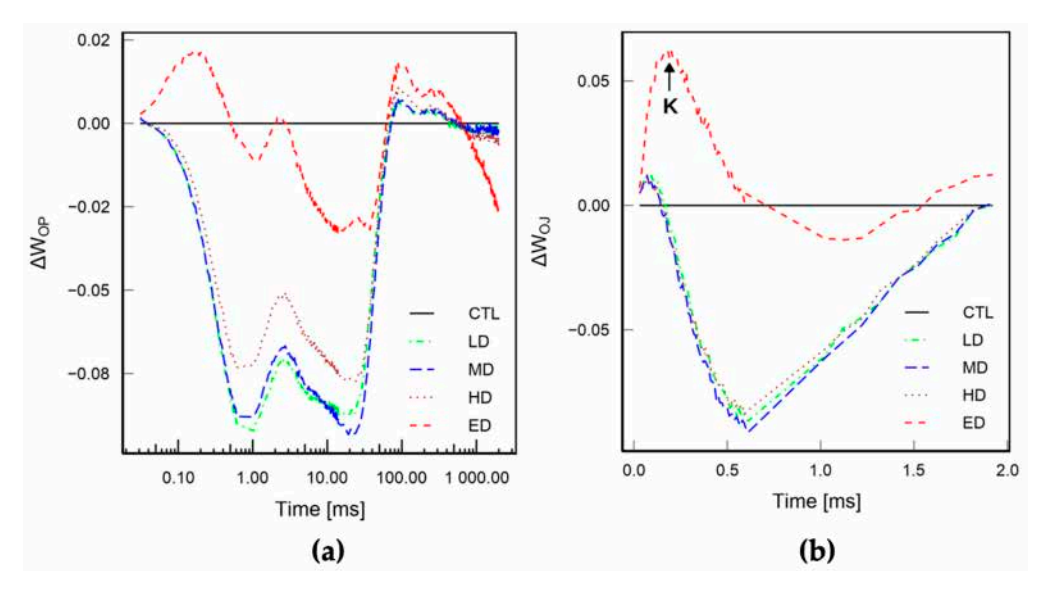


Figure 3. (a) Relative variable fluorescence of *Cladocopium goreaui* from O-Step to P-Step (W_{OP}) and (b) Relative variable fluorescence from O-Step to J-step (W_{OJ}) of *Cladocopium goreaui* exposed to different concentrations of *Arthrospira platensis* extract: control (CTL), low dose (LD), medium dose (MD), high dose (HD), and extreme dose (ED). The K letter indicates the K-peak inflection.

Phycology **2025**, 5, 50 7 of 16

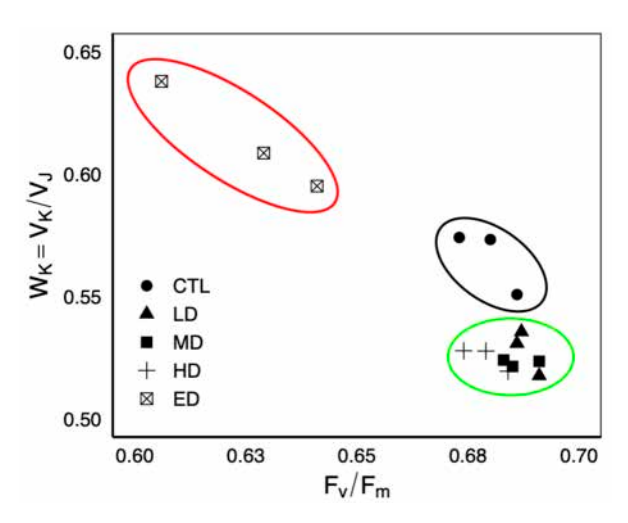


Figure 4. Amplitude of K-step ($W_k = V_k/V_j$) as a function of the parameter F_v/F_m in *Cladocopium goreaui* exposed to different concentrations of *Arthrospira platensis* extract. Ellipses represent segregated groups (green: positive impacts, black: control, red: negative impacts), but not statistical differences. Control (CTL), low dose (LD), medium dose (MD), high dose (HD), and extreme dose (ED).

When examining V_k/V_j ratio as a function of F_v/F_m , three distinct groups appeared, illustrated by colored ellipses (ellipses did not indicate any statistical significance) (Figure 4). The ED group was segregated from other treatments, including the control one, by a higher V_k/V_j ratio and a lower F_v/F_m . Interestingly, V_k/V_j ratios for LD, MD, and HD treatments were lower than those of the control one, forming two additional groups with negligible variations in F_v/F_m . In all treatments, F_v/F_m values were above 0.5, with ED values (0.62 \pm 0.01) being lower than LD (0.68 \pm 0.00, p = 0.012).

3.3. Parameters Extracted from JIP Transient

All parameters (n = 13) extracted from the OJIP analysis showed significant differences between treatments. However, statistical differences were not systematically observed between the control condition and treatments, but rather within treatments, especially between the two smallest concentrations (LD, MD), which displayed comparable values, and the highest one (ED), which statistically differed from them (Table 3).

The relative fluorescence at the J-step (V_j) for LD was significantly reduced by 20% compared to the control (p=0.04) (Figure 2b and Table 3). Consequently, M_0 , the initial slope of the standardized transient (V_t) from the O-step to 300 μ s, was also affected by this reduction in V_j , though the effect was not significant (Table 3, p=0.054). Considering specific fluxes, ABS/RC, TR₀/RC, and DI₀/RC for MD were not significantly but rather slightly reduced by 10% compared to the control condition. ABS/RC, TR₀/RC, ET₀/RC, and DI₀/RC for ED, however, increased by 29, 17, 7, and 35% (p < 0.05) compared to MD, finally exceeding the control values (Table 3).

In contrast, efficiencies followed an opposite trend with φP_0 , ψE_0 , and φE_0 for ED being reduced by 8, 8, and 35%, respectively, compared to LD (p < 0.05). ψE_0 and φE_0 for LD were increased by 11 and 14% compared to the control, although they were not significant. φP_0 exhibited the lowest variations, with a maximum reduction of 7% for ED compared to the control.

By analyzing the variation coefficient of the parameters, the strongest variations were observed for Pi_Abs (30%). To characterize the relationship between Pi_Abs and the concentration, data were first modeled using linear or quadratic models (Figure 5). Based on the Akaike Information Criterion (AIC), the quadratic model provided the best fit for Pi_Abs, resulting in a concave parabolic curve where higher values corresponding to the best response. LD and MD induced an over-response up to 150%, which decreased with

Phycology **2025**, 5, 50 8 of 16

the increasing concentration to reach a 16% reduction at the ED concentration (Figure 5). Analysis revealed a non-linear relationship between the response and the logarithmic concentration within the experimental range. The curve (best described by the equation $y = -0.48x^2 - 6.03x + 138.83$) identified a maximum response at x = -6.28, corresponding to a real extract concentration of 0.018 mg L⁻¹.

Table 3. Chl *a* fluorescence parameters in *Cladocopium goreaui* exposed to different concentrations of *Arthrospira platensis* extract. Control (CTL), low dose (LD), medium dose (MD), high dose (HD), and extreme dose (ED). Values are mean \pm SD (n = 3). Letters correspond to statistical differences between treatments after post-hoc analysis.

	CTL	LD	MD	HD	ED
	Basic parameters calculated from the extracted transcient				
$\overline{F_0}$	13,600 ± 99 ab	$13,730 \pm 188$ ab	$13,665 \pm 211$ ab	13,925 ± 239 a	12,993 ± 500 b
F_{m}	42,448 \pm 724 $^{\mathrm{ab}}$	43,966 \pm 441 $^{\mathrm{a}}$	43 ,586 \pm 473 $^{\mathrm{ab}}$	$43,391 \pm 536$ ab	$34,700 \pm 915$ ^b
F_j	24,849 \pm 1377 $^{\mathrm{a}}$	23,278 \pm 254 $^{\mathrm{a}}$	23,256 \pm 262 $^{\mathrm{a}}$	$23,830 \pm 366$ a	21,327 \pm 511 $^{\mathrm{b}}$
$V_{\mathbf{j}}^{'}$	$0.39\pm0.05~^{\mathrm{a}}$	$0.32 \pm 0.00^{\ \mathrm{b}}$	0.32 ± 0.00 $^{\mathrm{ab}}$	0.34 ± 0.01 $^{ m ab}$	0.38 ± 0.01 a
$\dot{\mathrm{M_0}}$	0.83 ± 0.14 a	0.61 ± 0.02 a	0.61 ± 0.01 a	0.65 ± 0.02 a	0.87 ± 0.05 a
		Quantum yields	s and efficiencies		
$\varphi P_0 (=F_v/F_m)$	0.68 ± 0.01 ab	0.69 ± 0.00 a	0.69 ± 0.00 ab	0.68 ± 0.01 ab	0.63 ± 0.02 b
ψE_0	0.61 ± 0.05 a	$0.68 \pm 0.00^{\ \mathrm{b}}$	0.68 ± 0.00 $^{ m ab}$	$0.66\pm0.01~\mathrm{ab}$	0.62 ± 0.01 a
$arphi ext{E}_0$	0.41 ± 0.04 $^{ m ab}$	0.47 ± 0.00 a	0.47 ± 0.00 $^{ m ab}$	0.45 ± 0.01 $^{ m ab}$	$0.39 \pm 0.02^{\ \mathrm{b}}$
	Specific energy fluxes (per RC: Q_A^- reducing PSII reaction center) in ms ⁻¹				
ABS/RC	$3.11 \pm 0.13^{\text{ ab}}$	2.81 ± 0.07 ab	2.79 ± 0.01 a	$2.84 \pm 0.05 ~^{\mathrm{ab}}$	3.61 ± 0.24 b
Tr_0/RC	2.11 ± 0.07 ab	1.93 ± 0.04 $^{ m ab}$	1.92 ± 0.00 a	1.93 ± 0.02 $^{\mathrm{ab}}$	2.25 ± 0.08 ^b
Et_0/RC	1.29 ± 0.07 a	1.32 ± 0.02 $^{\mathrm{ab}}$	1.3 ± 0.01 a	1.28 ± 0.01 $^{\mathrm{ab}}$	1.39 ± 0.03 b
Di_0/RC	1.00 ± 0.06 $^{ m ab}$	0.88 ± 0.03 $^{ m ab}$	0.88 ± 0.01 a	$0.91\pm0.03~\mathrm{ab}$	1.35 ± 0.16 b
Performance index					
Pi_Abs	1.10 ± 0.34 ab	1.70 ± 0.08 a	1.66 ± 0.06 a	1.47 ± 0.12 ab	$0.75 \pm 0.13^{\text{ b}}$

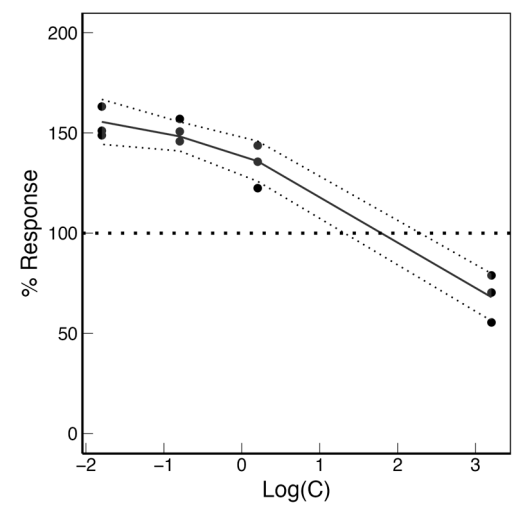


Figure 5. Performance Index (Pi_Abs) of *Cladocopium goreaui* exposed to increasing concentrations of *Arthrospira platensis* extract, expressed as percentage response of the control on a logarithmic scale. Black dots represent the response of each treatment relative to the control, expressed as the percentage difference. The black curve represents the fitted quadratic model associated with the data, and dotted lines correspond to the 95% confidence interval.

Phycology **2025**, 5, 50 9 of 16

4. Discussion

4.1. Physiological Response of C. goreaui to the A. platensis Extract

Based on growth rate data, the *Arthrospira platensis* extract at environmental concentrations (LD and MD) did not exhibit any signs of toxicity on the dinoflagellate *Cladocopium goreaui* after 7 days in culture. Conversely, with a concentration up to 10^5 the environmental one, the reduction of the maximum growth rate and the maximum cell concentration indicated a strong impact on the growth physiology of *C. goreaui* [42,43].

Unlike the impacts of herbicides [31], benzophenone-3 [27], copper [48], or microplastics [32], for which a reduction in the energy used for primary photochemistry has been demonstrated, our study did not reveal substantial differences in F_v/F_m , indicating that the impacts were located beyond PSII. These impacts were detected using fast chlorophyll, a fluorescence induction (OJIP), applied to coral endosymbionts, and which provides more detailed insights into the dynamics of electron transport. The PAM fluorometric approach (OJIP, RLC) revealed a biphasic response of microalgae Performance Index (Pi_Abs) to the extract. Pi_Abs is generally used as stress indicator for photosynthetic organisms [33,49,50] or as an indicator of adaptation to specific environments [51,52]. This index is the product of three distinct processes: the RC-active density (RC/ABS), the primary photochemistry efficiency (φP_0 also expressed as F_v/F_m), and the probability that a trapped electron goes beyond $Q_A^-(\psi E_0)$ [34,53]. Consequently, a small variation, positive or negative, of one of these parameters influences the Pi_Abs response and enables comparisons between experimental and control conditions. Pi_Abs changes have been shown to reveal early responses to certain specific stress such as drought, high temperature, or metal stress before visible alterations occur [51,54,55].

In this study, the microalgae Pi_Abs biphasic response to the extract is characterized by (1) an increase in energy conservation from photons absorbed by PSII to the reduction of intersystem electron acceptors at low doses (LD and MD), reaching a maximum at 0.018 mg L^{-1} , followed by (2) a decline in energy conservation to a "Zero Equivalent Point" (ZEP) at 108.8 mg L^{-1} . Beyond this threshold, which also corresponds to the No-Observed-Adverse-Effect-Level (NOAEL), adverse photophysiological effects occur on the PSII, primarily due to an impairment of the Oxygen Evolving Complex (OEC). This biphasic relation aligns with the hormetic principle described by Calabrese and Blain [56] and follows an "inverted U-shape curve" with a maximum at 157%, characteristic of a classic hormetic stimulatory response [57]. In the present study, the NOAEL is calculated at 108.8 mg L^{-1} , a concentration up to 10^4 times greater than those used in the cosmetic industry, suggesting that the extract toxicity only occurs at high doses up to 10^4 times greater than those used in the cosmetic industry [39].

4.2. Enhancement of the Photosynthetic Steps at Low Doses, Based on Absorption Basis

At low doses, the energy conservation is enhanced by two parameters of Pi_Abs : RC/ABS and ψE_o . (1) The increase of RC/ABS indicates a higher RC-active density of the biochemical complex [33], accompanied by a reduction in specific energy fluxes ABS, TR_0 , ET_0 , and DI_0 per active RC (i.e., Q_A -reducing RC). This suggests a reduction in the apparent antenna size indicating that the received energy is distributed among a greater number of active RCs [34,58]. Consequently, RCs receiving a lower amount of energy remain longer in their reduced state before being oxidized, thereby reducing their net closure rate (M_0) [33]. Interestingly, these adaptations are usually found when organisms have to cope with high light and regulate their RC density to prevent PSII photophysiological damages [55]. Here, low doses of A. platensis extracts would increase the light absorption efficiency of C. goreaui. (2) Once trapped in the Electron Transport Chain (ETC), electrons are then transported through the intersystem to reach the final electron acceptor: ferredoxin. In our

case, the yield of trapped electron transported beyond Q_A^- (ψE_0) is increased compared to a condition without the extract, which facilitates the reduction of the downstream ETC entities: Q_B , PQ, b_6/f , and PC. The electron transport yield (ϕE_0) is also increased due to the combination of ϕP_0 and ψE_0 , reflecting a higher quality of electron transport from the antenna to the intersystem of electron acceptors. Similarly, such improved electron transport efficiency is also found when photosynthetic organisms are exposed to substances with a protective role, such as antioxidants, allowing the quenching of oxygen reactive species (ROS) generated during the photosynthetic processes [58–61].

In this experiment, the increase in RC-active density and yield efficiencies at low doses could be attributed to the presence of micronutrients in the Arthrospira platensis extract. This cyanobacterium is known to be a source of trace elements such as manganese (Mn), iron (Fe), or copper (Cu) [62], which play important roles in photosynthesis or cellular repair mechanisms in algae [63,64]. In particular, Mn is involved in the OEC structure and also serves as a cofactor for the superoxide dismutase enzyme (SOD), which scavenges ROS [65]. In addition, A. platensis is also known to produce phycobiliproteins [66], specifically phycocyanin, which is concentrated at 1.1 g L^{-1} in the used extract, and may have an antioxidant effect on algae. In our case, given the hydrosoluble properties of phycocyanin, this pigment is unlikely to act directly as a protective antioxidant within the chloroplasts where photosynthesis takes place. However, its effects could be indirect. Although the precise mechanisms remain unclear, Xu et al. [67] suggested that exogenous phycocyanin enhanced the antioxidant enzymes activities in Arabidopsis thaliana. Similarly, Varia et al. [68] reported that lettuce grown on phycocyanin-rich soil exhibited a higher flavonoid content, which also contributes to the antioxidant response. These findings highlight the need for further mechanistic evaluation into the beneficial effects of such compounds for coral symbionts.

4.3. High-Dose Adverse Effects of Substances on Photophysiology

Conversely, at high doses beyond NOAEL, *A. platensis* extract induces adverse effects on *C. goreaui* photophysiology. Specifically, Pi_Abs at ED is reduced by a factor of two compared to the optimum (157 to 75% of the control condition) and by 30% compared to the control without extract. The apparent antenna size also undergoes modifications in the opposite way as low doses, as evidenced by the reduction in the fraction of active reaction centers (RC-active). With fewer active RCs, the absorption per RC increases, leading to higher specific fluxes (TR₀ and ET₀) and a saturation of oxidized RCs. As a result, the net closure rate of RCs increases, requiring them to dissipate excess energy (DI₀/RC) to prevent photodamage by heat or fluorescence under 2100 μ mol photons m⁻² s⁻¹. On the contrary, the absence of variation in non-photochemical quenching induced by RLC (NPQ_{ind}) between treatments, together with the absence of photoinhibition, indicates that light intensity at 1000 μ mol photons m⁻² s⁻¹ is not inhibitory to PSII [69].

While antenna modifications occur, primary photochemistry is slightly reduced, with φP_0 decreasing to 0.63, indicating a small reduction in the fraction of energy transferred to the electron transport chain (ETC). A decrease in φP_0 could result either from PSII impairment or from a slowdown in electron transport downstream in the ETC. In our case, φP_0 remains relatively high, suggesting that PSII is in a good functional state.

Nevertheless, the presence of a W_K/W_J ratio above 0.6 suggests an accumulation of reduced Q_A and highly fluorescent pheophytin (Pheo⁻) caused by electron limitation on the PSII donor side [70]. Strasser et al. [33] demonstrated that this limitation results from an alteration of the Oxygen-Evolving Complex (OEC), which is unable to supply enough electrons to the excited P680 (P680⁺), hindering its return to the ground state (P680). This creates a bottleneck at Pheo⁻, which can no longer transfer its electron to Q_A , and

consequently reduces electron transfer beyond Q_A^- (from Q_A to Q_B , and ultimately to NADPH). The impairment of the OEC and the PSII modifications finally participate to prompt a decrease in the maximum electron transport rate (rETR_m) in the ETC [71–73].

5. Conclusions

According to our results, different effects can be found following exposure to an *A. platensis* extract. At low doses, the extract (1) induces a reorganization of the apparent antenna size by increasing the fraction of RC-active as an adaptation to favorable environment and (2) supplies beneficial compounds that protect the ETC, enhancing the electron transport efficiency [63]. Conversely, at high dose, the extract (1) causes apparent antenna modifications to prevent photodamage, (2) alters the EOC due to an excess of ROS produced by excessive energy, (3) reduces the ETC performance, and consequently (4), limits growth of *C. goreaui*.

We show for the first time that a low concentration of *A. platensis* extract added to the culture medium of *C. goreaui* does not induce toxicity. On the contrary, this low dose enhances light absorption efficiency and electron transport, ultimately improving the algal Performance Index. Furthermore, this study assesses the ecotoxicological impact of an algal-based product at environmentally relevant concentrations, a key aspect given its inclusion in sunscreen formulations and the associated risks for coral reef ecosystems. Our study evaluated the exposure of the free-form of *C. goreaui* to different doses of extract. In view of these results, it is therefore essential to test these same doses on the symbiotic form of *C. goreaui* (inside the coral host) as well as on other symbiont genera, such as *Durusdinium*, which are also found in the eastern Pacific region [74]. Symbionts in culture exhibit a relatively similar physiological, morphological, and cellular cycle, while in hospite they display more heterogeneous cells according to their cellular cycle, potentially attenuating the effects of the commercial product.

Supplementary Materials: The following supporting information can be downloaded at: https://www.mdpi.com/article/10.3390/phycology5030050/s1, Table S1: Parameters extracted from Rapid Light Curves (RLC) modelized by Jassby and Platt model. rETR_m: maximum relative electron transport rate; Ik: rETR_m/ α , saturating point; α : ability to use low light intensities. p-values were obtained following a Kruskal–Wallis test. Table S2: Chl a fluorescence parameters in *Cladocopium goreaui* exposed to different concentrations of an 80% glycerol solution, matrix of the *Arthrospira platensis* extract. Control (CTL), low dose (LD), medium dose (MD), high dose (HD). Values are mean \pm SD (n = 3). p-values were obtained following a Kruskal–Wallis test. Figure S1: Pearson's correlation analysis between cell concentration (C) in cell mL $^{-1}$ and minimal fluorescence (F_0).

Author Contributions: Conceptualization, T.L.V.-C., F.H., T.J. and L.L.; Methodology, T.L.V.-C., F.H., T.J. and L.L.; Validation, F.H., T.J. and L.L.; Formal Analysis, T.L.V.-C. and T.J.; Investigation, T.L.V.-C., F.H., T.J. and L.L.; Resources, F.H. and T.J.; Data Curation, T.L.V.-C., F.H. and T.J.; Writing—Original Draft Preparation, T.L.V.-C.; Writing—Review and Editing, T.L.V.-C., F.H., T.J. and L.L.; Visualization, T.L.V.-C., F.H. and T.J.; Supervision, F.H. and T.J.; Project Administration, F.H. and L.L.; Funding Acquisition, F.H. and L.L. All authors have read and agreed to the published version of the manuscript.

Funding: T.L.V.-C. was beneficiary of a PhD grant (N° 400116/00) by URIAGE dermatological laboratories. Part of this work was also funded by IRD (PIGMENT project).

Institutional Review Board Statement: Not applicable.

Informed Consent Statement: Not applicable.

Data Availability Statement: Data will be made available on request.

Acknowledgments: The authors would like to thank Noémie Coulombier from the Technopole of New Caledonia for her technical support and for welcoming T.L.V.-C. to the LEMA laboratory.

Conflicts of Interest: The authors declare no conflicts of interest.

Abbreviations

The following abbreviations are used in this manuscript:

PAM	Pulse Amplificated Fluorometry
OJIP	JIP-test
RLC	Rapid Light Curve
ETC	Electron Transport Chain
PSII	Photosystem II
OEC	Oxygen Evolving Complex
PCP	Personal Care Product
UVF	Ultra-Violet Filter
ROS	Reactive oxygen species
PC	Phycocyanin
NPQ	Non-Photochemical Quenching
PAR	Photosynthetically Active Radiation
NOAEL	No Observed Adverse Effect Level

Appendix A

Appendix A.1

Table A1. Parameters, formulas and their definitions used in this study for the analysis of the Chl *a* fluorescence [34].

Parameter	Definition	Formula	Meaning	
	Basic fluorescence data measured or calculated from the JIP-test			
F_0	Minimal fluorescence after dark adaptation	F at 50 μs	Minimum fluorescence when all PSII RCs are open	
	Maximal fluorescence during a		Maximal fluorescence when all PSII	
F_{m}	saturating flash on dark adapted sample	F at P-step (peak)	RCs are closed (can be attributed to Fp)	
	Maximum fluorescence in a			
F _m ′	light-adapted sample under a saturating flash			
F_t	Fluorescence at time t			
F_{v}	Variable fluorescence	$\mathrm{F_{t}}-\mathrm{F}_{0}$		
$F_{\rm v}/F_{\rm m}$	Maximum quantum yield for primary photochemistry	$(F_{\rm m}-F_{\rm 0})/F_{\rm m}$	Maximum light utilization efficiency of PSII	
V_{t}	Relative variable fluorescence at time t	$(F_t - F_0)/(F_m - F_0)$	Relative fluorescence double normalized on F_m and F_0	
	Initial slope (in ms^{-1}) of the			
\mathbf{M}_0	fluorescent transcient normalized on the variable fluorescence (V_t)	$M_0 = [(\Delta F/\Delta t)_0]/(F_m - F_0)$	Q _A reduction rate	
	Biophysical parameters derived from the basic parameters by the JIP-test			
	Specific energy fluxes (per active RC: Q _A -reducing PSII reducing center)			

Table A1. Cont.

Parameter	Definition	Formula	Meaning		
ABS/RC	Absorption flux at the antenna per RC	$M_0\times (1/V_J)\times (1/\varphi P_0)$	PSII apparent antenna size. RC/ABS the reciprocal corresponds to the fraction of active RC per antenna.		
TR ₀ /RC	Trapped energy flux leading to Q_A reduction per active RC	$M_0 \times (1/V_J)$	The rate of which an electron is trapped in RC resulting in reduction of Q_A to Q_A^-		
ET ₀ /RC	Electron transport flux per active RC	$M_0\times (1/V_J)\times (1-V_J)$	The rate by which an electron moves from Q_A^- to PQ		
DI_0/RC	Dissipation flux into heat per active RC	$ABS/RC - TR_0/RC$			
	Quantui	m yields and efficiencies			
$\overline{\phi P_0}$	Maximum quantum yield for primary photochemistry	$F_{\rm v}/F_{\rm m}$	Quantum yield for primary chemistry		
ϕE_0	Quantum yield for electron transport	$[1-(F_0/F_m)]\times (1-V_j)$			
ψE_0		$(1 - V_j)$	The probability that an electron moves further than Q_A^-		
	Pe	erformance index			
Pi_Abs	Performance index for energy conservation	$[RC/ABS] \times [\varphi P_0/(1 - \varphi P_0)] \times [\psi E_0/(1 - \psi E_0)]$	Performance index for energy conservation from a photon absorbed by PSII until the reduction of intersystem electron acceptors		
RLC measured and extracted parameters					
rETR	Relative electron transport rate	$PAR \times QY \times 0.5 \times 0.84$			
$rETR_{max}$	Maximum relative electron transport rate		rETR levelling at a maximum light-saturated rate		
α	Initial RLC slope, maximal light use coefficient for PSII		Ability to use low light intensities		
Ik	Light saturating index [μ mol photon m ⁻² s ⁻¹]	$Ik = rETR_{max}/\alpha$	Ability to use high light intensities		
NPQ _{ind}	Induced Non Photochemical Quenching during RLC experiment	$(F_m - F_t)/(F_t)$	Ability to dissipate energy into heat as a protective mechanism. Stern-Volmer coefficient		

References

- LaJeunesse, T.C.; Parkinson, J.E.; Gabrielson, P.W.; Jeong, H.J.; Reimer, J.D.; Voolstra, C.R.; Santos, S.R. Systematic Revision of Symbiodiniaceae Highlights the Antiquity and Diversity of Coral Endosymbionts. *Curr. Biol.* 2018, 28, 2570–2580.e6. [CrossRef] [PubMed]
- 2. Muscatine, L. The Role of Symbiotic Algae in Carbon and Energy Flux in Reef Corals. Coral Reefs 1990, 25, 75.
- 3. Burke, L.M. Reefs at Risk Revisited; World Resources Institute: Washington, DC, USA, 2011; ISBN 978-1-56973-762-0.
- 4. Hughes, T.P.; Kerry, J.T.; Álvarez-Noriega, M.; Álvarez-Romero, J.G.; Anderson, K.D.; Baird, A.H.; Babcock, R.C.; Beger, M.; Bellwood, D.R.; Berkelmans, R.; et al. Global Warming and Recurrent Mass Bleaching of Corals. *Nature* **2017**, *543*, 373–377. [CrossRef]
- 5. Hoegh-Guldberg, O.; Andréfouët, S.; Fabricius, K.E.; Diaz-Pulido, G.; Lough, J.; Marshall, P.A.; Pratchett, M.S. Vulnerability of Coral Reefs in the Tropical Pacific to Climate Change. In *Vulnerability of Tropical Pacific Fisheries and Aquaculture to Climate Change*; Secretariat of the Pacific Community: Noumea, New Caledonia, 2011; Volume 49.
- 6. Sánchez-Quiles, D.; Blasco, J.; Tovar-Sánchez, A. Sunscreen Components Are a New Environmental Concern in Coastal Waters: An Overview. In *The Handbook of Environmental Chemistry*; Springer: Berlin/Heidelberg, Germany, 2020.
- 7. Gaw, S.; Thomas, K.V.; Hutchinson, T.H. Sources, Impacts and Trends of Pharmaceuticals in the Marine and Coastal Environment. *Phil. Trans. R. Soc. B* **2014**, *369*, 20130572. [CrossRef]

Phycology **2025**, 5, 50 14 of 16

8. Watkins, Y.S.D.; Sallach, J.B. Investigating the Exposure and Impact of Chemical UV Filters on Coral Reef Ecosystems: Review and Research Gap Prioritization. *Integr. Envir Assess. Manag.* **2021**, *17*, 967–981. [CrossRef]

- 9. D'Amico, M.; Kallenborn, R.; Scoto, F.; Gambaro, A.; Gallet, J.C.; Spolaor, A.; Vecchiato, M. Chemicals of Emerging Arctic Concern in North-Western Spitsbergen Snow: Distribution and Sources. *Sci. Total Environ.* **2024**, *908*, 168401. [CrossRef]
- 10. Apel, C.; Joerss, H.; Ebinghaus, R. Environmental Occurrence and Hazard of Organic UV Stabilizers and UV Filters in the Sediment of European North and Baltic Seas. *Chemosphere* **2018**, 212, 254–261. [CrossRef]
- 11. Downs, C.A.; Bishop, E.; Diaz-Cruz, M.S.; Haghshenas, S.A.; Stien, D.; Rodrigues, A.M.S.; Woodley, C.M.; Sunyer-Caldú, A.; Doust, S.N.; Espero, W.; et al. Oxybenzone Contamination from Sunscreen Pollution and Its Ecological Threat to Hanauma Bay, Oahu, Hawaii, U.S.A. *Chemosphere* 2022, 291, 132880. [CrossRef] [PubMed]
- 12. Mitchelmore, C.L.; He, K.; Gonsior, M.; Hain, E.; Heyes, A.; Clark, C.; Younger, R.; Schmitt-Kopplin, P.; Feerick, A.; Conway, A.; et al. Occurrence and Distribution of UV-Filters and Other Anthropogenic Contaminants in Coastal Surface Water, Sediment, and Coral Tissue from Hawaii. *Sci. Total Environ.* **2019**, *670*, 398–410. [CrossRef]
- 13. Mitchelmore, C.L.; Burns, E.E.; Conway, A.; Heyes, A.; Davies, I.A. A Critical Review of Organic Ultraviolet Filter Exposure, Hazard, and Risk to Corals. *Environ. Toxicol. Chem.* **2021**, 40, 967–988. [CrossRef]
- 14. Stien, D.; Suzuki, M.; Rodrigues, A.M.S.; Yvin, M.; Clergeaud, F.; Thorel, E.; Lebaron, P. A Unique Approach to Monitor Stress in Coral Exposed to Emerging Pollutants. *Sci. Rep.* **2020**, *10*, 9601. [CrossRef]
- Downs, C.A.; Kramarsky-Winter, E.; Segal, R.; Fauth, J.; Knutson, S.; Bronstein, O.; Ciner, F.R.; Jeger, R.; Lichtenfeld, Y.; Woodley, C.M.; et al. Toxicopathological Effects of the Sunscreen UV Filter, Oxybenzone (Benzophenone-3), on Coral Planulae and Cultured Primary Cells and Its Environmental Contamination in Hawaii and the U.S. Virgin Islands. Arch. Environ. Contam. Toxicol. 2016, 70, 265–288. [CrossRef] [PubMed]
- 16. Fel, J.-P.; Lacherez, C.; Bensetra, A.; Mezzache, S.; Béraud, E.; Léonard, M.; Allemand, D.; Ferrier-Pagès, C. Photochemical Response of the Scleractinian Coral Stylophora Pistillata to Some Sunscreen Ingredients. *Coral Reefs* **2019**, *38*, 109–122. [CrossRef]
- 17. He, T.; Tsui, M.M.P.; Tan, C.J.; Ng, K.Y.; Guo, F.W.; Wang, L.H.; Chen, T.H.; Fan, T.Y.; Lam, P.K.S.; Murphy, M.B. Comparative Toxicities of Four Benzophenone Ultraviolet Filters to Two Life Stages of Two Coral Species. *Sci. Total Environ.* **2019**, *651*, 2391–2399. [CrossRef]
- 18. He, T.; Tsui, M.M.P.; Tan, C.J.; Ma, C.Y.; Yiu, S.K.F.; Wang, L.H.; Chen, T.H.; Fan, T.Y.; Lam, P.K.S.; Murphy, M.B. Toxicological Effects of Two Organic Ultraviolet Filters and a Related Commercial Sunscreen Product in Adult Corals. *Environ. Pollut.* 2019, 245, 462–471. [CrossRef] [PubMed]
- 19. Wijgerde, T.; van Ballegooijen, M.; Nijland, R.; van der Loos, L.; Kwadijk, C.; Osinga, R.; Murk, A.; Slijkerman, D. Adding Insult to Injury: Effects of Chronic Oxybenzone Exposure and Elevated Temperature on Two Reef-Building Corals. *Sci. Total Environ.* **2020**, 733, 139030. [CrossRef]
- 20. Danovaro, R.; Bongiorni, L.; Corinaldesi, C.; Giovannelli, D.; Damiani, E.; Astolfi, P.; Greci, L.; Pusceddu, A. Sunscreens Cause Coral Bleaching by Promoting Viral Infections. *Environ. Health Perspect.* **2008**, *116*, 441–447. [CrossRef]
- 21. Muscatine, L.; Porter, J.W. Reef Corals: Mutualistic Symbioses Adapted to Nutrient-Poor Environments. *BioScience* **1977**, 27, 454–460. [CrossRef]
- 22. Downs, C.A.; Fauth, J.E.; Halas, J.C.; Dustan, P.; Bemiss, J.; Woodley, C.M. Oxidative Stress and Seasonal Coral Bleaching. *Free Radic. Biol. Med.* 2002, 33, 533–543. [CrossRef]
- 23. Burns, E.E.; Davies, I.A. Coral Ecotoxicological Data Evaluation for the Environmental Safety Assessment of Ultraviolet Filters. *Environ. Toxic. Chem.* **2021**, *40*, 3441–3464. [CrossRef]
- 24. Vuckovic, D.; Tinoco, A.I.; Ling, L.; Renicke, C.; Pringle, J.R.; Mitch, W.A. Conversion of Oxybenzone Sunscreen to Phototoxic Glucoside Conjugates by Sea Anemones and Corals. *Science* 2022, 376, 644–648. [CrossRef] [PubMed]
- 25. Salvi, L.; Niccolai, A.; Cataldo, E.; Sbraci, S.; Paoli, F.; Storchi, P.; Rodolfi, L.; Tredici, M.R.; Mattii, G.B. Effects of Arthrospira Platensis Extract on Physiology and Berry Traits in Vitis Vinifera. *Plants* **2020**, *9*, 1805. [CrossRef]
- Moeller, M.; Pawlowski, S.; Petersen-Thiery, M.; Miller, I.B.; Nietzer, S.; Heisel-Sure, Y.; Kellermann, M.Y.; Schupp, P.J. Challenges in Current Coral Reef Protection—Possible Impacts of UV Filters Used in Sunscreens, a Critical Review. Front. Mar. Sci. 2021, 8, 665548. [CrossRef]
- 27. Zhang, K.; Shen, Z.; Yang, W.; Guo, J.; Yan, Z.; Li, J.; Lin, J.; Cao, X.; Tang, J.; Liu, Z.; et al. Unraveling the Metabolic Effects of Benzophenone-3 on the Endosymbiotic Dinoflagellate *Cladocopium Goreaui*. Front. Microbiol. 2023, 13, 1116975. [CrossRef] [PubMed]
- Butler, C.C.; Turnham, K.E.; Lewis, A.M.; Nitschke, M.R.; Warner, M.E.; Kemp, D.W.; Hoegh-Guldberg, O.; Fitt, W.K.; Van Oppen, M.J.H.; LaJeunesse, T.C. Formal Recognition of Host-generalist Species of Dinoflagellate (*Cladocopium*, Symbiodiniaceae) Mutualistic with Indo-Pacific Reef Corals. *J. Phycol.* 2023, 59, 698–711. [CrossRef]
- 29. Alessi, C.; Lemonnier, H.; Camp, E.F.; Wabete, N.; Payri, C.; Rodolfo Metalpa, R. Algal Symbiont Diversity in Acropora Muricata from the Extreme Reef of Bouraké Associated with Resistance to Coral Bleaching. *PLoS ONE* **2024**, *19*, e0296902. [CrossRef]

Phycology **2025**, 5, 50 15 of 16

30. Quigley, K.M.; Alvarez Roa, C.; Beltran, V.H.; Leggat, B.; Willis, B.L. Experimental Evolution of the Coral Algal Endosymbiont, *Cladocopium goreaui*: Lessons Learnt across a Decade of Stress Experiments to Enhance Coral Heat Tolerance. *Restor. Ecol.* **2021**, 29, e13342. [CrossRef]

- 31. Marzonie, M.; Flores, F.; Sadoun, N.; Thomas, M.C.; Valada-Mennuni, A.; Kaserzon, S.; Mueller, J.F.; Negri, A.P. Toxicity Thresholds of Nine Herbicides to Coral Symbionts (Symbiodiniaceae). *Sci. Rep.* **2021**, *11*, 21636. [CrossRef]
- 32. Liang, J.; Niu, T.; Zhang, L.; Yang, Y.; Li, Z.; Liang, Z.; Yu, K.; Gong, S. Polystyrene Microplastics Exhibit Toxic Effects on the Widespread Coral Symbiotic *Cladocopium Goreaui*. *Environ*. *Res.* **2025**, 268, 120750. [CrossRef]
- 33. Strasser, R.J.; Tsimilli-Michael, M.; Srivastava, A. Analysis of the Chlorophyll a Fluorescence Transient. In *Chlorophyll a Fluorescence*; Papageorgiou, G.C., Govindjee, Eds.; Advances in Photosynthesis and Respiration; Springer: Dordrecht, The Netherlands, 2004; Volume 19, pp. 321–362, ISBN 978-1-4020-3217-2.
- 34. Tsimilli-Michael, M. Special Issue in Honour of Prof. Reto J. Strasser—Revisiting JIP-Test: An Educative Review on Concepts, Assumptions, Approximations, Definitions and Terminology. *Photosynthetica* **2020**, *58*, 275–292. [CrossRef]
- 35. Labille, J.; Slomberg, D.; Catalano, R.; Robert, S.; Apers-Tremelo, M.-L.; Boudenne, J.-L.; Manasfi, T.; Radakovitch, O. Assessing UV Filter Inputs into Beach Waters during Recreational Activity: A Field Study of Three French Mediterranean Beaches from Consumer Survey to Water Analysis. *Sci. Total Environ.* 2020, 706, 136010. [CrossRef] [PubMed]
- 36. Poiger, T.; Buser, H.-R.; Balmer, M.E.; Bergqvist, P.-A.; Müller, M.D. Occurrence of UV Filter Compounds from Sunscreens in Surface Waters: Regional Mass Balance in Two Swiss Lakes. *Chemosphere* **2004**, *55*, 951–963. [CrossRef]
- 37. Milinkovitch, T.; Vacher, L.; Le Béguec, M.; Petit, E.; Dubillot, E.; Grimmelpont, M.; Labille, J.; Tran, D.; Ravier, S.; Boudenne, J.-L.; et al. Sunscreen Use during Recreational Activities on a French Atlantic Beach: Release of UV Filters at Sea and Influence of Air Temperature. *Environ. Sci. Pollut. Res.* 2024, 31, 41046–41058. [CrossRef] [PubMed]
- 38. Ficheux, A.S.; Chevillotte, G.; Wesolek, N.; Morisset, T.; Dornic, N.; Bernard, A.; Bertho, A.; Romanet, A.; Leroy, L.; Mercat, A.C.; et al. Consumption of Cosmetic Products by the French Population Second Part: Amount Data. *Food Chem. Toxicol.* **2016**, *90*, 130–141. [CrossRef] [PubMed]
- 39. Joly, F.; Branka, J.-E.; Darnis, E.; Lefeuvre, L. Telomere Protective Effects of a Cyanobacteria Phycocyanin against Blue Light and UV Irradiations: A Skin Anti-Aging and Photo-Protective Agent. *J. Cosmet. Dermatol. Sci. Appl.* **2019**, *09*, 336–345. [CrossRef]
- 40. Guillard, R.R.L.; Hargraves, P.E. Stichochrysis Immobilis Is a Diatom, Not a Chrysophyte. *Phycologia* 1993, 32, 234–236. [CrossRef]
- 41. Chakravarti, L.J.; Beltran, V.H.; Van Oppen, M.J.H. Rapid Thermal Adaptation in Photosymbionts of Reef-building Corals. *Glob. Change Biol.* **2017**, 23, 4675–4688. [CrossRef]
- 42. Jauffrais, T.; Agogué, H.; Gemin, M.-P.; Beaugeard, L.; Martin-Jézéquel, V. Effect of Bacteria on Growth and Biochemical Composition of Two Benthic Diatoms Halamphora Coffeaeformis and Entomoneis Paludosa. *J. Exp. Mar. Biol. Ecol.* 2017, 495, 65–74. [CrossRef]
- 43. Coulombier, N.; Blanchier, P.; Le Dean, L.; Barthelemy, V.; Lebouvier, N.; Jauffrais, T. The Effects of CO₂-Induced Acidification on Tetraselmis Biomass Production, Photophysiology and Antioxidant Activity: A Comparison Using Batch and Continuous Culture. *J. Biotechnol.* **2021**, 325, 312–324. [CrossRef]
- 44. Sibat, M.; Mai, T.; Chomérat, N.; Bilien, G.; Lhaute, K.; Hess, P.; Séchet, V.; Jauffrais, T. Gambierdiscus Polynesiensis from New Caledonia (South West Pacific Ocean): Morpho-Molecular Characterization, Toxin Profile and Response to Light Intensity. *Harmful Algae* 2025, 145, 102859. [CrossRef]
- 45. Jassby, A.D.; Platt, T. Mathematical Formulation of the Relationship between Photosynthesis and Light for Phytoplankton: Photosynthesis-Light Equation. *Limnol. Oceanogr.* **1976**, *21*, 540–547. [CrossRef]
- 46. Ralph, P.J.; Gademann, R. Rapid Light Curves: A Powerful Tool to Assess Photosynthetic Activity. *Aquat. Bot.* **2005**, *82*, 222–237. [CrossRef]
- 47. Oukarroum, A.; Madidi, S.E.; Schansker, G.; Strasser, R.J. Probing the Responses of Barley Cultivars (*Hordeum vulgare* L.) by Chlorophyll a Fluorescence OLKJIP under Drought Stress and Re-Watering. *Environ. Exp. Bot.* **2007**, *60*, 438–446. [CrossRef]
- 48. Tang, J.; Cai, W.; Yan, Z.; Zhang, K.; Zhou, Z.; Zhao, J.; Lin, S. Interactive Effects of Acidification and Copper Exposure on the Reproduction and Metabolism of Coral Endosymbiont *Cladocopium Goreaui*. *Mar. Pollut. Bull.* **2022**, 177, 113508. [CrossRef] [PubMed]
- 49. Gan, T.; Yin, G.; Zhao, N.; Tan, X.; Wang, Y. A Sensitive Response Index Selection for Rapid Assessment of Heavy Metals Toxicity to the Photosynthesis of Chlorella Pyrenoidosa Based on Rapid Chlorophyll Fluorescence Induction Kinetics. *Toxics* 2023, 11, 468. [CrossRef] [PubMed]
- 50. Pavlović, I.; Mlinarić, S.; Tarkowská, D.; Oklestkova, J.; Novák, O.; Lepeduš, H.; Bok, V.V.; Brkanac, S.R.; Strnad, M.; Salopek-Sondi, B. Early Brassica Crops Responses to Salinity Stress: A Comparative Analysis Between Chinese Cabbage, White Cabbage, and Kale. Front. Plant Sci. 2019, 10, 450. [CrossRef]
- 51. Antunović Dunić, J.; Mlinarić, S.; Pavlović, I.; Lepeduš, H.; Salopek-Sondi, B. Comparative Analysis of Primary Photosynthetic Reactions Assessed by OJIP Kinetics in Three Brassica Crops after Drought and Recovery. *Appl. Sci.* **2023**, *13*, 3078. [CrossRef]

52. Mlinarić, S.; Žuna Pfeiffer, T.; Krstin, L.; Špoljarić Maronić, D.; Ožura, M.; Stević, F.; Varga, M. Adaptation of Amorpha Fruticosa to Different Habitats Is Enabled by Photosynthetic Apparatus Plasticity. *Photosynthetica* **2021**, *59*, 137–147. [CrossRef]

- 53. Strasser, R.J.; Srivastava, A.; Tsimilli-Michael, M. The Fluorescence Transient as a Tool to Characterize and Screen Photosynthetic Samples. *Probing Photosynth. Mech. Regul. Adapt.* **2000**, 25, 445–483.
- 54. Kumar, D.; Singh, H.; Raj, S.; Soni, V. Chlorophyll a Fluorescence Kinetics of Mung Bean (*Vigna radiata* L.) Grown under Artificial Continuous Light. *Biochem. Biophys. Rep.* **2020**, 24, 100813. [CrossRef]
- 55. Kalaji, H.M.; Carpentier, R.; Allakhverdiev, S.I.; Bosa, K. Fluorescence Parameters as Early Indicators of Light Stress in Barley. *J. Photochem. Photobiol. B Biol.* **2012**, 112, 1–6. [CrossRef] [PubMed]
- 56. Calabrese, E.; Blain, R. The Occurrence of Hormetic Dose Responses in the Toxicological Literature, the Hormesis Database: An Overview. *Toxicol. Appl. Pharmacol.* **2005**, 202, 289–301. [CrossRef]
- 57. Calabrese, E.J.; Blain, R.B. The Hormesis Database: The Occurrence of Hormetic Dose Responses in the Toxicological Literature. *Regul. Toxicol. Pharmacol.* **2011**, *61*, 73–81. [CrossRef] [PubMed]
- 58. Wu, P.; Ma, Y.; Ahammed, G.J.; Hao, B.; Chen, J.; Wan, W.; Zhao, Y.; Cui, H.; Xu, W.; Cui, J.; et al. Insights into Melatonin-Induced Photosynthetic Electron Transport under Low-Temperature Stress in Cucumber. Front. Plant Sci. 2022, 13, 1029854. [CrossRef] [PubMed]
- 59. Pospíšil, P. Production of Reactive Oxygen Species by Photosystem II. *Biochim. Biophys. Acta (BBA)-Bioenerg.* **2009**, *1787*, 1151–1160. [CrossRef]
- 60. Chen, X.; Zhou, Y.; Cong, Y.; Zhu, P.; Xing, J.; Cui, J.; Xu, W.; Shi, Q.; Diao, M.; Liu, H. Ascorbic Acid-Induced Photosynthetic Adaptability of Processing Tomatoes to Salt Stress Probed by Fast OJIP Fluorescence Rise. Front. Plant Sci. 2021, 12, 594400. [CrossRef]
- 61. Oukarroum, A.; Bussotti, F.; Goltsev, V.; Kalaji, H.M. Correlation between Reactive Oxygen Species Production and Photochemistry of Photosystems I and II in *Lemna gibba* L. Plants under Salt Stress. *Environ. Exp. Bot.* 2015, 109, 80–88. [CrossRef]
- 62. Rahim, A.; Çakir, C.; Ozturk, M.; Şahin, B.; Soulaimani, A.; Sibaoueih, M.; Nasser, B.; Eddoha, R.; Essamadi, A.; El Amiri, B. Chemical Characterization and Nutritional Value of Spirulina Platensis Cultivated in Natural Conditions of Chichaoua Region (Morocco). S. Afr. J. Bot. 2021, 141, 235–242. [CrossRef]
- 63. Smythers, A.L.; Crislip, J.R.; Slone, D.R.; Flinn, B.B.; Chaffins, J.E.; Camp, K.A.; McFeeley, E.W.; Kolling, D.R.J. Excess Manganese Increases Photosynthetic Activity via Enhanced Reducing Center and Antenna Plasticity in Chlorella Vulgaris. *Sci. Rep.* **2023**, 13, 11301. [CrossRef]
- 64. Singh, H.; Kumar, D.; Soni, V. Performance of Chlorophyll a Fluorescence Parameters in Lemna Minor under Heavy Metal Stress Induced by Various Concentration of Copper. *Sci. Rep.* **2022**, *12*, 10620. [CrossRef]
- 65. Biscéré, T.; Ferrier-Pagès, C.; Gilbert, A.; Pichler, T.; Houlbrèque, F. Evidence for Mitigation of Coral Bleaching by Manganese. *Sci. Rep.* **2018**, *8*, 16789. [CrossRef]
- 66. Fernandes, R.; Campos, J.; Serra, M.; Fidalgo, J.; Almeida, H.; Casas, A.; Toubarro, D.; Barros, A.I.R.N.A. Exploring the Benefits of Phycocyanin: From Spirulina Cultivation to Its Widespread Applications. *Pharmaceuticals* **2023**, *16*, 592. [CrossRef]
- 67. Xu, Q.; Zhu, T.; Zhao, R.; Zhao, Y.; Duan, Y.; Liu, X.; Luan, G.; Hu, R.; Tang, S.; Ma, X.; et al. Arthrospira Promotes Plant Growth and Soil Properties under High Salinity Environments. *Front. Plant Sci.* **2023**, *14*, 1293958. [CrossRef] [PubMed]
- 68. Varia, J. Biostimulation with Phycocyanin-Rich Spirulina Extract in Hydroponic Vertical Farming. *Sci. Hortic.* **2022**, 299, 111042. [CrossRef]
- 69. Mériot, V.; Roussel, A.; Brunet, N.; Chomerat, N.; Bilien, G.; Le Déan, L.; Berteaux-Lecellier, V.; Coulombier, N.; Lebouvier, N.; Jauffrais, T. Heterocapsa Cf. Bohaiensis (Dinoflagellate): Identification and Response to Nickel and Iron Stress Revealed through Chlorophyll a Fluorescence. *Photosynthetica* **2024**, 62, 27. [CrossRef] [PubMed]
- 70. Brestic, M.; Zivcak, M.; Kalaji, H.M.; Carpentier, R.; Allakhverdiev, S.I. Photosystem II Thermostability in Situ: Environmentally Induced Acclimation and Genotype-Specific Reactions in *Triticum aestivum* L. *Plant Physiol. Biochem.* **2012**, *57*, 93–105. [CrossRef]
- 71. Shanker, A.K.; Amirineni, S.; Bhanu, D.; Yadav, S.K.; Jyothilakshmi, N.; Vanaja, M.; Singh, J.; Sarkar, B.; Maheswari, M.; Singh, V.K. High-Resolution Dissection of Photosystem II Electron Transport Reveals Differential Response to Water Deficit and Heat Stress in Isolation and Combination in Pearl Millet [Pennisetum glaucum (L.) R. Br.]. Front. Plant Sci. 2022, 13, 892676. [CrossRef]
- 72. Stefanov, M.A.; Rashkov, G.D.; Yotsova, E.K.; Borisova, P.B.; Dobrikova, A.G.; Apostolova, E.L. Different Sensitivity Levels of the Photosynthetic Apparatus in *Zea mays* L. and *Sorghum bicolor* L. under Salt Stress. *Plants* **2021**, *10*, 1469. [CrossRef]
- 73. Zhu, Y.; Lin, Q.; Yang, Y.; Xia, Y.; Cai, H.; Feng, X.; Gonçalves, R.J.; Guan, W. Ocean Acidification Enhances the Tolerance of Dinoflagellate Prorocentrum Donghaiense to Nanoplastic-Induced Oxidative Stress by Modulating Photosynthetic Performance. *Front. Mar. Sci.* **2024**, *11*, 1494930. [CrossRef]
- 74. Tanvet, C.; Camp, E.F.; Sutton, J.; Houlbrèque, F.; Thouzeau, G.; Rodolfo-Metalpa, R. Corals Adapted to Extreme and Fluctuating Seawater PH Increase Calcification Rates and Have Unique Symbiont Communities. *Ecol. Evol.* **2023**, *13*, e10099. [CrossRef]

Disclaimer/Publisher's Note: The statements, opinions and data contained in all publications are solely those of the individual author(s) and contributor(s) and not of MDPI and/or the editor(s). MDPI and/or the editor(s) disclaim responsibility for any injury to people or property resulting from any ideas, methods, instructions or products referred to in the content.